Analysis of detection error for spot position in fiber nutation model

Xueqiang Zhao (赵学强)[1,2,3], Yunpeng Zhang (张云鹏)[1,2], Minjie Huang (黄敏捷)[3], Peipei Hou (侯培培)[1], Ren Zhu (朱 韧)[3], Jianfeng Sun (孙建锋)[1,2], Xia Hou (侯 霞)[2,3,*], and Weibiao Chen (陈卫标)[1,2,]**

[1]*Key Laboratory of Space Laser Communication and Detection Technology, Shanghai Institute of Optics and Fine Mechanics, Chinese Academy of Sciences, Shanghai 201800, China*

[2]*Center of Materials Science and Optoelectronics Engineering, University of Chinese Academy of Sciences, Beijing 100049, China*

[3]*Laboratory of Space Laser Engineering, Shanghai Institute of Optics and Fine Mechanics, Chinese Academy of Sciences, Shanghai 201800, China*

**Corresponding author: hou_xia@siom.ac.cn; **corresponding author: wbchen@siom.ac.cn*

Received August 22, 2019; accepted November 14, 2019; posted online February 8, 2020

The influences of nutation trail accuracy, simplification of coupling model, spot position jitter, and power variation of incident light on the detection error are analyzed theoretically. Under the condition of satisfying the requirements, the nutation radius is less than 1.13 μm, the accuracy of the nutation trail is less than 0.04 μm, and the detection range is [−5 μm, +5 μm]. The nutation frequency is 160 times spot position jitter frequency and 100 times intensity jitter frequency of incident light. The analysis is of great significance for determining nutation radius and frequency in the tracking system based on fiber nutation.

Keywords: fiber nutation; detection error; tracking system.

doi: 10.3788/COL202018.020604.

In the inter-satellite laser communication system, the premise of ensuring the coupling efficiency of signal light to a single-mode fiber (SMF) is to obtain a stable receiving line of sight (LOS)[1]. The classical LOS stabilization tracking system calculates the boresight error by detecting the target spot position on the sensitive surface of the spot position detector (SPD), in which the communication LOS and the tracking LOS are strictly coaxial[2]. Practically, the misalignment of the optical path makes the tracking LOS and communication LOS incompletely coincide, which leads to the decrease of coupling efficiency in the tracking process.

The tracking system based on fiber nutation overcomes the shortcomings of the classical tracking system, which directly uses the signal light to solve the boresight error. The communication LOS and the tracking LOS coincide completely, and the tracking reference point is stable. In 1989, Swanson *et al.* first proposed to use fiber nutation to solve the boresight error and simplify the structure of the tracking system, in which a voice coil motor is used to drive the SMF. Due to the technical limitation of the driver, it is difficult to further reduce the volume of the fiber nutation device[3]. In 1992, Knibbe *et al.* used the method of electro-optic scanning for nutation signal light in the propagation path. It has the advantage of high nutation frequency and can improve the detection frequency, but the insertion loss of the electro-optic crystal is large[4]. In 2016, Gao *et al.* used a similar method to solve the boresight error by using a fast steering mirror (FSM) for nutation signal light[5]. In 2017, they used a piezoelectric ceramic tube for nutation of the end face of the SMF instead of the voice coil motor mentioned above, which can reduce the volume of the nutation component[6]. In 2018, Li *et al.* proposed a coarse and fine tracking method based on fiber nutation to increase the detection field of view (FOV)[7]. In 2019, Chen *et al.* reported a fiber nutation tracking system based on coherent detection, which has higher detection sensitivity than direct detection[8]. In the same year, we proposed an engineering scheme of fiber nutation tracking technology. The system uses an erbium-doped fiber amplifier (EDFA) to amplify the signal light, reducing the sensitivity of the signal demodulation module to the insertion loss and the requirement of gain bandwidth product of the photo-detector[9].

In this Letter, considering the application background of inter-satellite laser communication, the influences of nutation trail repetition accuracy, simplification of coupling model, spot position jitter, and power variation of incident light on the detection error are analyzed, and a mathematical model for the calculation error is established. We give the design constraints of the fiber nutation module quantitatively by numerical simulation.

Figure 1 shows the principle block diagram of the tracking system based on fiber nutation. The nutation device drives the end face of the SMF to scan the spot periodically at the focal plane. The algorithm execution unit demodulates the boresight error synchronously according to the nutation position signal and the intensity envelope fluctuation signal and then controls the FSM to track the incident light. The demodulation and feedback control process are implemented in the field-programmable gate array (FPGA) device.

 © 2020 Chinese Optics Letters

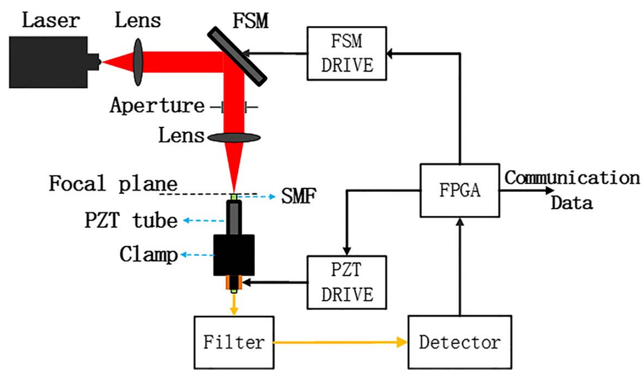

Fig. 1. Principle of fiber nutation tracking system based on direct detection.

At present, there are two methods for calculating the boresight error: the "stochastic parallel gradient descent (SPGD) algorithm" and the "four-point scanning algorithm"[5,6,9,10]. The SPGD algorithm relies on multiple iterations, which makes it difficult to improve the control bandwidth. In this Letter, the "four-point scanning algorithm" is used to explain the principle of fiber nutation. Figure 2 shows the principle diagram of the "four-point scanning algorithm", in which the end face of the fiber scans the spot counterclockwise. In each nutation cycle, the moments corresponding to the intersection $[(X+,0), (0,Y+), (X-,0), (0,Y-)]$ of the nutation trail and coordinate axis are nT, $nT+T/4$, $nT+T/2$ and $nT+3T/4$. The alignment deviation of light spot is expressed as[9]

$$\begin{cases} \rho_x = \frac{\omega_0^2}{4r}\ln\left[\frac{P(nT)}{P(nT+T/2)}\right], \\ \rho_y = \frac{\omega_0^2}{4r}\ln\left[\frac{P(nT+T/4)}{P(nT+3T/4)}\right]. \end{cases} \tag{1}$$

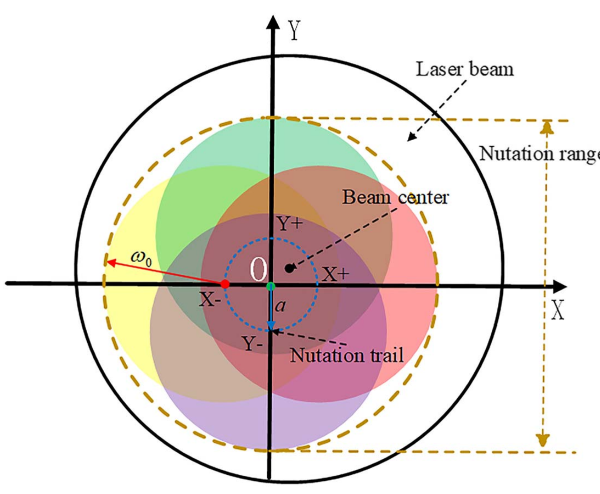

Fig. 2. Principle of "four-point scanning algorithm". The area in the black circle is the spot mode field at the focal plane, the blue circle is the nutation trail, and the area in the brown circle is the scanning range of fiber nutation. The red, green, yellow, and purple circles represent the positions of the end face of the SMF when nutation trail coincides with the coordinate axis, respectively.

where (ρ_x, ρ_y) is the position of the incident light spot, ω_0 is the mode field radius of the SMF, r is the fiber nutation radius, and $P(\cdot)$ is the optical power coupled into SMF corresponding to time t.

Fiber nutation radius r in Eq. (1) is an important parameter for the tracking system based on fiber nutation, which is determined according to the design requirement of link margin. The signal light receiving system can be simplified as a thin lens[11]. When satisfying the requirement of optimum aperture ratio, the coupling efficiency of space light into the SMF can be approximately expressed as[12]

$$\eta(\rho) = \eta_{\max}\exp\left(-\frac{\rho^2}{\omega_0^2}\right), \tag{2}$$

where ρ is the radial offset of the light spot from the SMF core, given by $\rho^2 = \rho_x^2 + \rho_y^2$.

When the center of the spot mode field coincides with the center of the nutation trail, there exists a transverse offset and an axial angular deviation. According to the geometric relationship, the transverse offset is equal to the nutation radius. When the axial angle deviation is small, the main factor affecting the coupling efficiency is lateral offset, and the coupling efficiency can be expressed as

$$\eta(r) = \eta_{\max}\exp\left(-\frac{r^2}{\omega_0^2}\right). \tag{3}$$

To measure the effect of the nutation radius on the coupling efficiency, the loss coefficient of coupling efficiency is defined as

$$\kappa(r) = \frac{\eta(0) - \eta(r)}{\eta(0)}. \tag{4}$$

Assuming that the laser communication link requires that the loss coefficient should be less than κ_m, the fiber nutation radius r satisfies the equation as follows by substituting Eq. (3) into Eq. (4):

$$r \le \omega_0\left[\ln\left(\frac{1}{1-\kappa_m}\right)\right]^{1/2}. \tag{5}$$

Figure 3 shows the loss of coupling efficiency as a function of nutation radius r. The larger the radius r, the more loss of coupling efficiency. When $r/\omega_0 < 0.2265$, the loss coefficient was less than 5%, and it was insensitive to the nutation radius. In the following analysis, the receiving fiber of the tracking system is a 1550 nm SMF ($\omega_0 = 5\,\mu m$), and the nutation radius is calculated as 1 μm.

Using Eq. (1) to calculate the boresight error requires that the spot position and power do not change in a fiber nutation period, which is difficult to meet in the process of a real inter-satellite laser communication environment.

The transmission of signal light follows the law of far-field diffraction: the tilting of the transmitter only changes

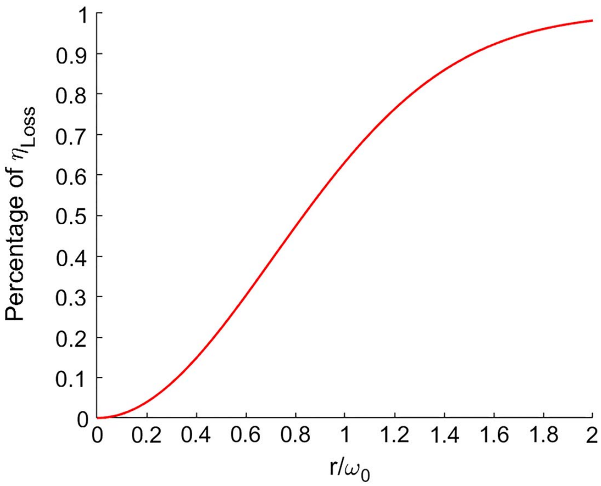

Fig. 3. Loss of coupling efficiency as a function of nutation radius.

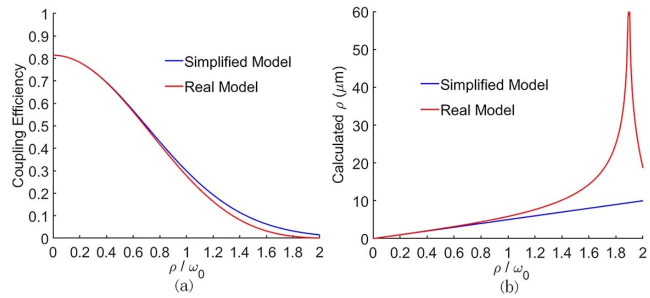

Fig. 4. (a) and (b) are the coupling efficiency and the calculated boresight error as a function of the real boresight error under the simplified model and real model.

the power in the aperture of the receiving terminal and has no effect on the detection of boresight error. The tracking error of the receiving terminal is completely determined by the tilting of the receiving terminal[13]. Therefore, under the condition of dynamic tracking, the position and power of the incident light spot at the focal plane will change dynamically, which will affect the accuracy of the spot position calculation. In addition, the simplification of the coupling model and the trail repetition accuracy also affect the calculation error.

The calculation error caused by model simplification is due to the use of a simplified coupling efficiency model from spatial light to SMF in the derivation process. Equation (2) is an approximate expression of coupling efficiency; the real coupling efficiency is expressed as[11]

$$\eta(\rho)_{\mathrm{real}} = \frac{8\left|\int_\epsilon^1 \beta \exp\left(-\beta^2 r'^2\right) J_0\left(2\frac{\beta\rho r'}{\omega_0}\right) r' \mathrm{d}r'\right|^2}{1-\epsilon^2}, \tag{6}$$

where ϵ is the occlusion ratio of the optical system. Here, occlusion is not considered, so $\epsilon = 0$. For an optimized optical system, $\beta = \pi R\omega_0/\lambda f = 1.12$. According to the coupling efficiency model by Eq. (6), the calculated boresight error is expressed as

$$\rho_{\mathrm{real}} = \frac{\omega_0^2}{4r}\ln\left[\frac{\eta(\rho+r)_{\mathrm{real}}}{\eta(\rho-r)_{\mathrm{real}}}\right]. \tag{7}$$

Figure 4(a) shows the coupling efficiency as a function of boresight error under the simplified model and the real model. Figure 4(b) shows the calculated boresight error as a function of real boresight error by using two models when the fiber nutation radius is 1 μm. When $\rho/\omega_0 < 0.6$, the coupling efficiency curve in the simplified model coincides with that in the real model. In the range of $0.6 < \rho/\omega_0 < 1.8$, the coupling efficiency in the real model drops faster, and the ratio of $\eta(\rho-r)_{\mathrm{real}}$ to $\eta(\rho+r)_{\mathrm{real}}$ becomes larger, which eventually leads to the increase of the calculation error. When $\rho/\omega_0 > 1.8$, the two coupling efficiency curves coincide gradually, so the calculation error decreases. The calculation error reaches the maximum value when $\rho/\omega_0 = 1.9$. The simulation results show that using Eq. (1) to calculate the boresight error leads to a large calculation error, especially when the offset $\rho > \omega_0$. Therefore, when the fiber nutation device is used in engineering without non-linear correction, the detection FOV should be limited to $[-\omega_0, +\omega_0]$.

The fiber nutation trail is not an ideal circle; its radius will change randomly and is slightly affected by mechanical vibration and electronic noise. Generally, the fiber nutation radius satisfies the Gauss distribution law mathematically, which is given by

$$P_d(r) = \frac{1}{\sqrt{2\pi}\sigma}\exp\left[-\frac{(r-\bar{r})^2}{2\sigma^2}\right]. \tag{8}$$

The fiber nutation radius is the statistical mean of the test results and satisfies $\bar{r} = 1\,\mu\mathrm{m}$. For a single measurement, the range of nutation radius r is $(\bar{r}-3\sigma, \bar{r}+3\sigma)$. In the worst case, the optical power corresponding to the sampling time is expressed as

$$\begin{cases} P(nT) = P_{\mathrm{in}}\eta_{\max}\exp\left[-\frac{(\rho_x-\bar{r}-3\sigma)^2}{\omega_0^2}\right], \\ P(nT+T/2) = P_{\mathrm{in}}\eta_{\max}\exp\left[-\frac{(\rho_x+\bar{r}+3\sigma)^2}{\omega_0^2}\right]. \end{cases} \tag{9}$$

Substituting Eqs. (9) into Eq. (1), the calculation error is expressed as

$$\Delta_t = \frac{3\rho_x\sigma}{\bar{r}}. \tag{10}$$

If the relative calculation error Δ_t/ρ_x caused by trail repetition accuracy is less than 10%, the control accuracy of the nutation radius is required to satisfy

$$\sigma < \frac{1}{30}\bar{r}. \tag{11}$$

Note that the ellipticity of the circle trail will also affect the calculation error in theory, but the constant coefficients of the Eq. (1) corresponding to the X and Y axes in the real system are independently calibrated. According to the centrosymmetric characteristic of the elliptic trail, the X axis and Y axis are independent, so the calculation error can be eliminated by correcting the coefficients separately.

The premise of determining the nutation frequency and amplitude is to evaluate the influence of spot position jitter on the calculation error. Our main concern is what conditions are satisfied for nutation frequency and spot jitter characteristics, so the calculation error can be reduced to an acceptable level (generally, the calculation error is less than 10%).

Under the condition of dynamic tracking, the position jitter of the incident light spot in the FOV of the fiber nutation tracking system can be seen as a combination of vibrations in different directions, which is expressed as

$$\overrightarrow{s(t)} = \sum_{k=1}^{n} \overrightarrow{A_k} \cos(2\pi f_k t + \varphi_k), \tag{12}$$

where A_k, f_k, and φ_k are the amplitude, frequency, and phase of the spot position jitter, respectively, and n represents the total number of vibration components.

Taking the X-axis motion as an example, the spot displacement projected onto the X axis is expressed as

$$s(t)_x = \sum_{k=1}^{n} |\overrightarrow{A_k}| \cos(\theta_k) \cos(2\pi f_k t + \varphi_k), \tag{13}$$

where θ_k is the angle between the fractional vibration and the X axis.

To simplify the model, we use the highest frequency of vibration noise to evaluate the boresight error; the movement of the spot on the X axis is expressed as

$$s(t)_x = |\overrightarrow{A_H}| \cos(\theta_H) \cos(2\pi f_H t + \varphi_H). \tag{14}$$

In the worst case, the direction of motion coincides with the X axis ($\theta_i = 0$), and the vibration has the greatest influence on the calculation of the boresight error. Calculating the differential of Eq. (9), the maximum velocity of the spot motion is expressed as

$$v_{\max} = 2\pi f_H A_H, \tag{15}$$

where A_H and f_H are the amplitude and frequency of spot position jitter, respectively. Considering the time period from nT to $nT + T/2$, the displacement of the spot along the X axis can be expressed as

$$\Delta s = v_{\max} \cdot \frac{1}{2f_n} = \frac{\pi A_H f_H}{f_n}, \tag{16}$$

where f_n is the fiber nutation frequency.

Substituting Eq. (16) into Eq. (2), optical power coupled into the SMF is expressed as

$$\begin{cases} P(nT) = P_{\text{in}}\eta_{\max} \exp\left[-\frac{(\rho_x - r)^2}{\omega_0^2}\right], \\ P(nT + T/2) = P_{\text{in}}\eta_{\max} \exp\left[-\frac{(\rho_x + r \pm \Delta s)^2}{\omega_0^2}\right]. \end{cases} \tag{17}$$

Substituting Eqs. (17) and (16) into Eq. (1), the calculated boresight error under the condition of spot jitter is expressed as

$$\rho_x^J = \left[\left(\rho_x + r \pm \frac{\pi A_H f_H}{f_n}\right)^2 - (\rho_x - r)^2\right] \Big/ 4r, \tag{18}$$

where ρ_x^J is the calculated boresight error in the X axis, and "±" represent the relationship between the spot vibration direction and the boresight error direction. '+' represents the same direction, and '−' represents the opposite direction.

By simplifying Eq. (18), the relative calculation error is expressed as

$$\begin{cases} \Delta_{J+} = \frac{\pi^2 A_H^2}{4r\alpha^2} + \frac{\rho_x \pi A_H}{2r\alpha} + \frac{\pi A_H}{2\alpha}, \\ \Delta_{J-} = \frac{\pi^2 A_H^2}{4r\alpha^2} - \frac{\rho_x \pi A_H}{2r\alpha} - \frac{\pi A_H}{2\alpha}, \end{cases} \tag{19}$$

where $\alpha = f_n/f_H$ and is defined as the relative nutation rate.

Equation (19) shows that the calculation error caused by spot jitter is related to the alignment deviation, jitter amplitude, and relative nutation rate when the nutation radius is determined. By comparing the two items in Eq. (19), the calculation error is larger when the vibration direction and the alignment deviation direction are the same. If the angle range corresponding to the maximum coupling efficiency of $1/e$ is defined as the FOV, the range of ρ_x is between 0 and 5 μm. In the dynamic tracking state, the spot jitters in the FOV with A_H ranging from 0 to 5 μm.

Figure 5 shows the calculation error as a function of the relative nutation rate when the jitter amplitudes are 2 μm,

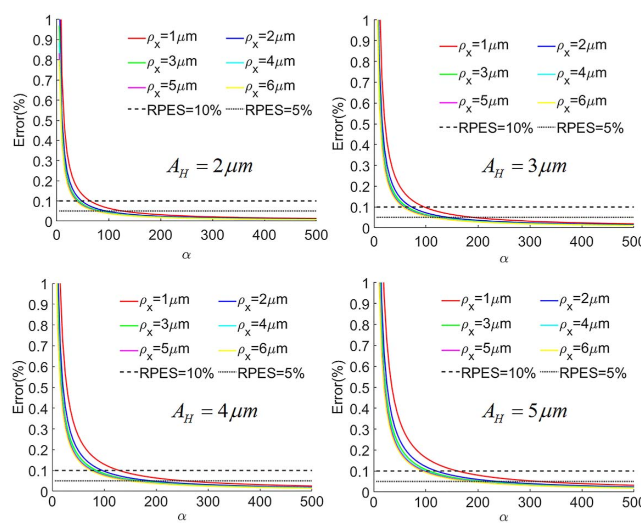

Fig. 5. Calculation error as a function of the relative nutation rate with different jitter amplitudes.

3 μm, 4 μm, and 5 μm, respectively, and the black dotted line is the reference position error standard (RPES). The results show that the calculation error decreases with the increase of the relative nutation rate. The larger the amplitude of spot jitter, the higher the relative nutation rate required. In the worst case, when the relative nutation rate is greater than 160, the calculation error is less than 10%, and, when the relative nutation rate is greater than 300, the calculation error is less than 5%.

The calculation error introduced by power jitter of incident light is also an important reference for determining nutation frequency. The FOV of the tracking system based on fiber nutation can be estimated by formula $\theta_n = \omega_0 / f_L M_T$, where f_L is the equivalent focal length of the fiber nutation receiving system, and M_T is the magnification factor of telescope. The pointing deviation is less than θ_n and vibrates near the tracking point. To simplify the model, the pointing error is expressed as $\theta(t) = \theta_A \sin(2\pi f_A t)$, where $\theta_A \le \theta_n$, and θ_A and f_A are the amplitude and frequency of the pointing deviation, respectively. The loss caused by pointing deviation is given by $L(\theta) = \exp(-8\theta^2/\theta_v^2)$, where θ_v is the beam divergence angle. In the worst case, the power in the receiving aperture is approximately expressed as

$$P(t)_{\text{in}} = \frac{P_{\max}}{2}[1 + L(\theta_A)] + \frac{P_{\max}}{2}[1 - L(\theta_A)]\sin(4\pi f_A t + \varphi_{\text{ape}}), \tag{20}$$

where φ_{ape} is the phase of power jitter in the receiving aperture.

When the incident light power changes, the power in Eq. (1) is expressed as

$$\begin{cases} P(nT) = P(nT)_{\text{in}}\eta(nT), \\ P(nT + T/2) = P(nT + T/2)_{\text{in}}\eta(nT + T/2). \end{cases} \tag{21}$$

Substituting Eq. (21) into Eq. (1), the calculation error is expressed as

$$\Delta_{\text{tm}} = \frac{\omega_0^2}{4r}\ln\left[\frac{P(nT)_{\text{in}}}{P(nT + T/2)_{\text{in}}}\right]. \tag{22}$$

Substituting Eq. (21) into Eq. (22),

$$\Delta_{\text{tm}} = \frac{\omega_0^2}{4r}\ln\left\{\frac{[1 + L(\theta_A)] + [1 - L(\theta_A)]\sin(4\pi f_A t)}{[1 + L(\theta_A)] + [1 - L(\theta_A)]\sin\left(4\pi f_A t + \frac{2\pi}{\beta}\right)}\right\}, \tag{23}$$

where $\beta = f_n / f_A$.

Equation (23) shows that the calculation error is related to θ_A/θ_v and β. The numerical simulation of the system is carried out under the critical working condition, where the parameters $\theta_v = 24$ μrad and $f_A = 200$ Hz. Figure 6 shows the calculation error as a function of β when the vibration amplitude θ_A is 3 μrad, 5 μrad, 7 μrad, and 9 μrad. When β is greater than 100, the calculation error is less than 0.3 μm in the worst case. It can also be seen that the calculation error caused by power jitter of incident light has no relation with the boresight error.

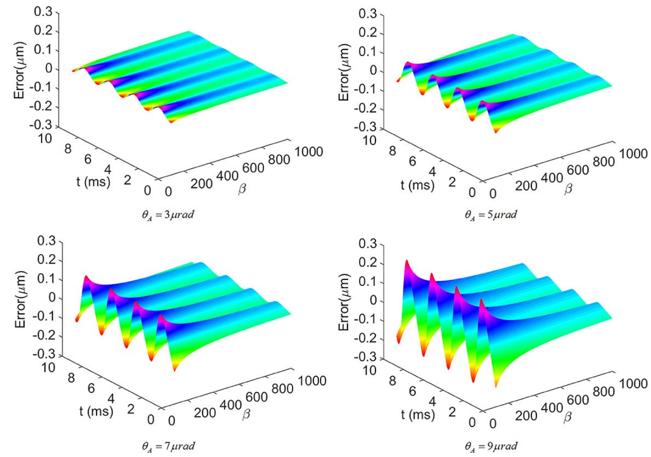

Fig. 6. Calculation error as a function of θ_A/θ_v and β.

In conclusion, the simplified coupling efficiency model, the trail repetition accuracy, the position, and power jitter of the incident light will affect the calculation error of the spot position. According to the analysis results, the detection FOV of the fiber nutation system should be limited to a range of $[-\omega_0, +\omega_0]$, and the fiber nutation radius should be 1/5 of the mode radius of the SMF. Under the worst conditions, the fiber nutation frequency should be 160 times greater than the spot position jitter frequency and 100 times greater than the power jitter frequency. The analysis methods and results are of great reference significance for the design of the fiber nutation tracking system.

References

1. J. H. Ji, J. J. Zhang, B. Wu, K. Wang, and M. Xu, Chin. Opt. Lett. **17**, 080604 (2019).
2. X. Yang, S. B. Wei, S. S. Kou, F. Yuan, and E. Cheng, Chin. Opt. Lett. **17**, 090604 (2019).
3. E. A. Swanson and R. S. Bondurant, Proc. SPIE **1218**, 13 (1990).
4. T. E. Knibbe, E. A. Swanson, and J. K. Roberge, Proc. SPIE **1635**, 309 (1992).
5. J. Q. Gao, J. F. Sun, J. W. Li, R. Zhu, P. P. Hou, and W. B. Chen, Chin. J. Lasers **43**, 0801001 (2016).
6. H. Y. He, J. F. Sun, Y. Zhou, Z. Y. Lu, Q. Xu, G. Zhang, G. Y. Li, M. M. Xu, B. Zhang, C. Z. Lao, and L. R. Liu, Proc. SPIE **10408**, 1040816 (2017).
7. B. Li, Y. T. Liu, S. F. Tong, L. Zhang, and H. F. Yao, IEEE Photon. J. **10**, 7909412 (2018).
8. M. Chen, C. Liu, D. M. Rui, and H. Xian, Opt. Commun. **430**, 223 (2019).
9. X. Q. Zhao, X. Hou, F. N. Zhu, T. Li, J. F. Sun, R. Zhu, M. Gao, Y. Yang, and W. B. Chen, Opt. Express **27**, 23996 (2019).
10. G. Huang, C. Geng, F. Li, and X. Y. Li, Chin. J. Lasers **44**, 0406001 (2017).
11. M. Toyoshima, J. Opt. Soc. Am. A **23**, 2246 (2006).
12. O. Wallner, P. J. Winzer, and W. R. Leeb, Appl. Opt. **41**, 637 (2002).
13. L. Liu, L. J. Wang, Z. Luan, J. F. Sun, A. Li, and D. Liu, Proc. SPIE **6304**, 63040C (2006).